Taylor & Francis
Taylor & Francis Group

Phase Transitions
A Multinational Journal

ISSN: 0141-1594 (Print) 1029-0338 (Online) Journal homepage: http://www.tandfonline.com/loi/gpht20

Ferronematics based on the nematic 6CB in combined electric and magnetic fields

V. Gdovinová, N. Tomašovičová, N. Éber, P. Salamon, T. Tóth-Katona, V. Závišová, J. Kováč, J. Jadžyn & P. Kopčanský

To cite this article: V. Gdovinová, N. Tomašovičová, N. Éber, P. Salamon, T. Tóth-Katona, V. Závišová, J. Kováč, J. Jadžyn & P. Kopčanský (2017) Ferronematics based on the nematic 6CB in combined electric and magnetic fields, Phase Transitions, 90:8, 780-789, DOI: 10.1080/01411594.2017.1286489

To link to this article: http://dx.doi.org/10.1080/01411594.2017.1286489

PHASE TRANSITIONS, 2017
VOL. 90, NO. 8, 780–789
http://dx.doi.org/10.1080/01411594.2017.1286489

Taylor & Francis
Taylor & Francis Group

Ferronematics based on the nematic 6CB in combined electric and magnetic fields

V. Gdovinová[a], N. Tomašovičová[a], N. Éber[b], P. Salamon[b], T. Tóth-Katona[b], V. Závišová[a], J. Kováč[a], J. Jadżyn[c] and P. Kopčanský[a]

[a]Institute of Experimental Physics, Slovak Academy of Sciences, Kosice, Slovakia; [b]Institute for Solid State Physics and Optics, Wigner Research Centre for Physics, Hungarian Academy of Sciences, Budapest, Hungary; [c]Institute of Molecular Physics, Polish Academy of Sciences, Poznan, Poland

ABSTRACT

This work is devoted to the study of composite systems of the liquid crystal 4-*n*-hexyl-4-cyanobiphenyl (6CB) doped with differently shaped magnetite nanoparticles. The ferronematic samples were prepared with the volume concentration of $\phi = 10^{-5}$ of spherical, as well as of rod-like magnetic particles. The structural transitions in ferronematic samples were observed by capacitance measurements in a capacitor made of indium-tin-oxide-coated glass electrodes in combined electric and magnetic fields.

ARTICLE HISTORY
Received 28 October 2016
Accepted 12 January 2017

KEYWORDS
Liquid crystals; magnetic particles; ferronematics; magnetic field

1. Introduction

The combination of fluidity of ordinary liquids with the direction-dependent electric and optical properties of crystalline solids make liquid crystals (LCs) attractive for the use in various commercial exploitations. Anisotropy in mechanical, electrical and magnetic properties permits LCs to be easily oriented, realigned or deformed by electric or magnetic field, by heating, or by mechanical stresses. These materials have attracted great attention for many practical applications in LC display industry [1], in photonics [2] and magneto-optics [3], in nanosensing and biosensing [4]. The search for new materials with exotic properties and for new technologies continues, in order to comply with the needs of the above, and other novel applications.

Thermotropic LCs are compounds whose liquid crystalline properties are induced purely by temperature variation. They possess one or more mesophases at temperatures between their melting point, below which the material is a crystalline solid, and the clearing point, above which the material is an isotropic liquid with properties of a conventional liquid phase, characterized by random and isotropic molecular ordering. Since their discovery, many LC phases have been identified [5]. One of the mesophases is the nematic phase, in which molecules have no positional order but tend to point in the same direction (along the director $\vec{n}$).

One of the most important discoveries in the control of LCs by electric or magnetic fields was the threshold behaviour in the reorientational response of LCs. The effect was described by Fréedericksz and named after him as 'Fréedericksz transition' [6]. It laid the foundation for LC applications in modern technology. The dielectric anisotropy ϵ_a of LCs is relatively large, and the driving voltage of the order of a few volts is sufficient to control the orientational response. Although LCs can also be controlled by a magnetic field, the magnetic sensitivity is rather low (the anisotropy of the

CONTACT N. Tomašovičová nhudak@saske.sk

diamagnetic susceptibility χ_a is of the order of 10^{-7}). It usually requires very high magnetic induction strength, of the order of tesla, to trigger the reorientation in LCs [5].

Brochard and de Gennes suggested a method, which would increase the magnetic sensitivity of LCs. In 1970, they presented the first theory for colloids of ferromagnetic nanoparticles in nematic LCs–ferronematics (FNs) [7]. The most essential feature of FNs is a strong coupling between the magnetic particles (their magnetic moment $\vec{m}$) and the LC matrix (the director $\vec{n}$). This coupling ensures that the effect of the magnetic field on the particles will be transferred into the nematic host. The theory of Brochard and de Gennes [7] predicted a rigid anchoring of LC molecules on the surfaces of magnetic particles with $\vec{m} \parallel \vec{n}$. Based on the estimations given in [7], first lyotropic [8,9] and then thermotropic FNs [10] have been prepared and studied.

Later experiments on thermotropic FNs have indicated that besides the predicted $\vec{m} \parallel \vec{n}$ condition, the case of $\vec{m} \perp \vec{n}$ is also possible. Based on the experiments, Burylov and Raikher modified the theoretical description of FNs [11–13]. They considered a finite value of the surface density of the anchoring energy W at the nematic–magnetic particle boundary and defined a parameter ω as the ratio of the anchoring energy to the elastic energy of the LC due to the presence of the particles ($\omega = Wd/K$, where d is the size of the magnetic particles and K is the relevant orientational–elastic Frank modulus). The parameter ω defines the type of anchoring of nematic molecules on the surface of magnetic particles. For rigid anchoring $\omega \gg 1$, while the soft anchoring is characterized by $\omega \leq 1$. The latter type of anchoring permits both boundary conditions: $\vec{m} \perp \vec{n}$ and $\vec{m} \parallel \vec{n}$.

Since then, structural transitions have been investigated in FNs with different combinations of magnetic nanoparticles (MNPs) and host nematic LCs [14–18]. Optical properties of magnetic fluids and FNs, such as transmittance, birefringence as well as the figure of merit of optical properties have also been tuned by the concentration of magnetic particles and that of the LC [19,20]. In addition, a linear magnetodielectric [21] and magneto-optic [22,23] response has been detected in these systems at low magnetic fields. It has also been shown that the isotropic–nematic phase transition temperature in FNs may be influenced by the shape anisotropy, as well as by the volume concentration of the MNPs [24–26]. Doping LCs with small amount of MNPs can lead to the decrease as well as to the increase of the threshold of the magnetic Fréedericksz transition [15]. The present paper discusses the type of the anchoring between the MNPs and the LC molecules. Experimental observations on structural transitions in FNs based on the thermotropic LC 4-*n*-hexyl-4′-cyanobiphenyl (6CB) doped with MNPs of different size and shape is reported.

2. Materials and methods

The thermotropic LC matrix of the FNs, 6CB, ensures the high chemical stability and the convenient temperature range of the nematic phase [27]. The LC was doped with MNPs of spherical and rod-like shapes. The synthesis of the spherical MNPs was based on the co-precipitation method described in [15]. The rod-like MNPs were synthesized through hydrolysis of $FeCl_3$ and $FeSO_4$ solutions containing urea [16]. The morphology and size distribution of the prepared nanoparticles were determined by transmission electron microscopy [15]. The mean diameter of the spherical MNPs was $d = 10$ nm. The rod-like MNPs had the average diameter of $d = 11$ nm and the mean length was $l = 240$ nm. MNPs were coated with oleic acid as a surfactant to prevent their aggregation. The doping was done by adding MNPs suspended in a solvent to the LC in its isotropic phase under continuous stirring, and waiting till the solvent evaporates in the absence of a magnetic field, resulting in compensated FNs with a $\phi = 10^{-5}$ volume concentration of the MNPs. Recently, it has been shown [28] that such a composition (6CB with oleic acid covered Fe_3O_4 MNPs) results in a very stable suspension, in which no micron-sized aggregates were observed more than three years after the preparation even at $\phi > 10^{-5}$. The stability of our FNs is illustrated in Figure 1.

Structural transitions in FNs were monitored by capacitance measurements in a capacitor made of indium-tin-oxide-coated glass electrodes with the planar alignment of LC molecules, i.e. the director is initially parallel to the capacitor electrodes. The capacitor with the electrode area of

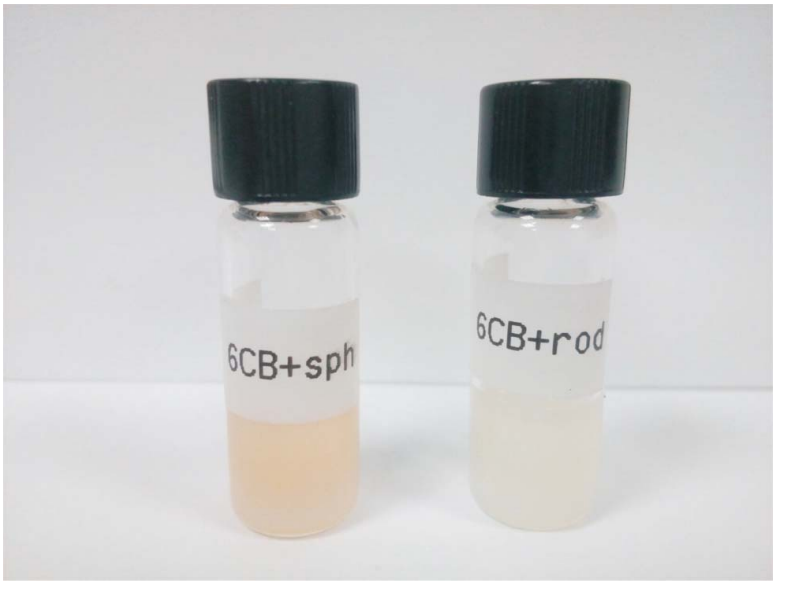

Figure 1. Pictures of ferronematics with spherical (left-hand side), and with rod-like (right-hand side) MNPs, taken about three months after the preparation.

approximately 1 cm × 1 cm has been placed into a thermostat system, regulated with the temperature stability of 0.05 °C, and the measurements have been done at the temperature of 23 °C. The distance between the electrodes (the sample thickness) was $D = 50$ μm. The capacitance C was measured at the frequency of 1 kHz by a TiePie Handyscope HS5 instrument, using sinusoidal voltage signal of root-mean-square value of U that was switched to the cell.

Structural transitions in FNs, provoked by combined electric and magnetic fields, have been investigated by the simultaneous application of a magnetic, and an ac electric field. The electric field generated by U was applied perpendicular to, while the magnetic field $\vec{H}$ (i.e. the magnetic induction $\vec{B} = \mu_0\vec{H}$) was parallel with the initial director orientation $\vec{n}$. In this geometry, the electric field destabilizes the initial director orientation, while the magnetic field acts against and tends to stabilize the initial (planar) state. Figure 2 shows the variation of the reduced capacitance $(C - C_0)/(C_{\max} - C_0)$ (where C, C_0 and $C_{\max}$ are the sample capacitance, its value at $U = 0$ and $U = 7.5$ V, respectively) with U for $H = 0$ in the undoped 6CB, indicating an electric field-induced splay Fréedericksz transition with a threshold voltage of $U_F = 0.75$ V. In Figure 2, the voltage dependence of the reduced capacitance of the FNs is also presented, demonstrating that in the absence of magnetic field, the electric Fréedericksz transition threshold is the same for all substances, i.e. $U_F = U_{Ffn} = 0.75$ V. All subsequent measurements were performed under the condition of $U > U_F$.

3. Experimental results

Magnetization curves of the nanoparticles are presented in Figure 3, and show that both spherical and rod-like MNPs exhibit superparamagnetic properties.

Magnetization curves of the undoped 6CB and of the two FNs, measured in the nematic phase (at $T = 23$ °C) are presented in Figure 4. The undoped 6CB exhibits the usual diamagnetic behaviour, while the FN composite with spherical MNPs, at low magnetic fields, behaves as a superparamagnet displaying no hysteresis. The diamagnetic features of the host matrix become dominating only at

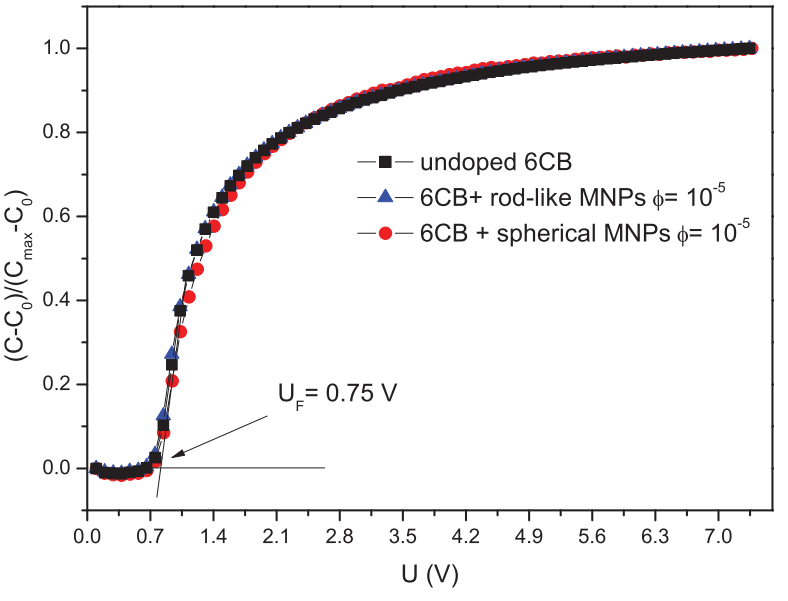

Figure 2. Dependence of the capacitance of the LC 6CB and of the FNs on the applied voltage U at $B = 0$, in the classical electric Fréedericksz transition. The thresholds are determined by linear extrapolation from the initial slope.

higher magnetic fields. Superparamagnetic features in the FN with rod-like MNPs are much less pronounced, presumably due to the low concentration of MNPs.

Figures 5–7 show how the reduced capacitance depends on the external magnetic induction B (which is related to H via the equation $B = \mu_0 H$; μ_0 is the permeability of vacuum) in the undoped 6CB, in 6CB doped with spherical, and in 6CB doped with rod-like MNPs, respectively, at various U voltages. Here C_0 and C_{max} are the capacitance values measured at $B = 0$ and at $B = B_{max} = 0.6$ T, respectively.

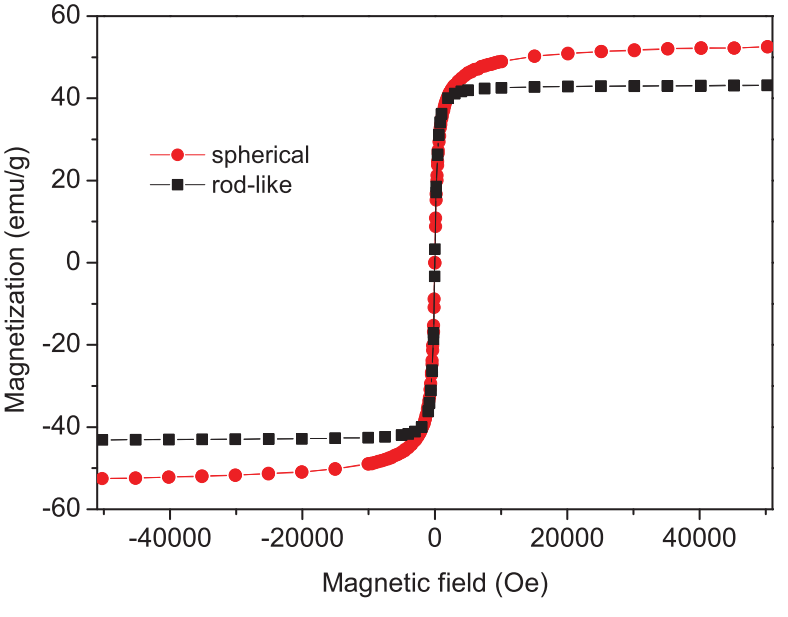

Figure 3. Magnetization curves of the spherical and rod-like MNPs.

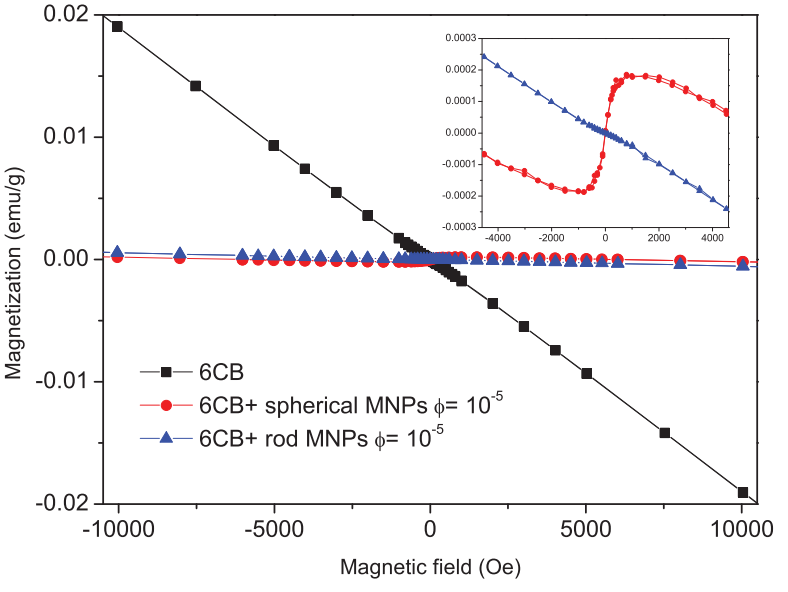

Figure 4. Magnetization curves of the undoped 6CB, and of 6CB doped with spherical, as well as with rod-like MNPs. The inset represents the blow-up for the two FNs in the low magnetic field region.

We emphasize again, that the U values in Figures 5–7 are larger than the Fréedericksz threshold voltage at $B = 0$ ($U_F = U_{Ffn}$ =0.75V). Therefore, U causes a deformed state approaching the homeotropic alignment, which is then destabilized by the magnetic field, and at high enough B values (above a critical magnetic induction B_c) the initial planar alignment is reobtained. B_c can be obtained from the voltage–capacitance curves by linear extrapolation, as illustrated in Figure 5 for $U = 1.0$ V. As one can see from Figures 5–7, the larger U shifts the required critical magnetic field B_c towards larger values in 6CB, as well as in both FNs.

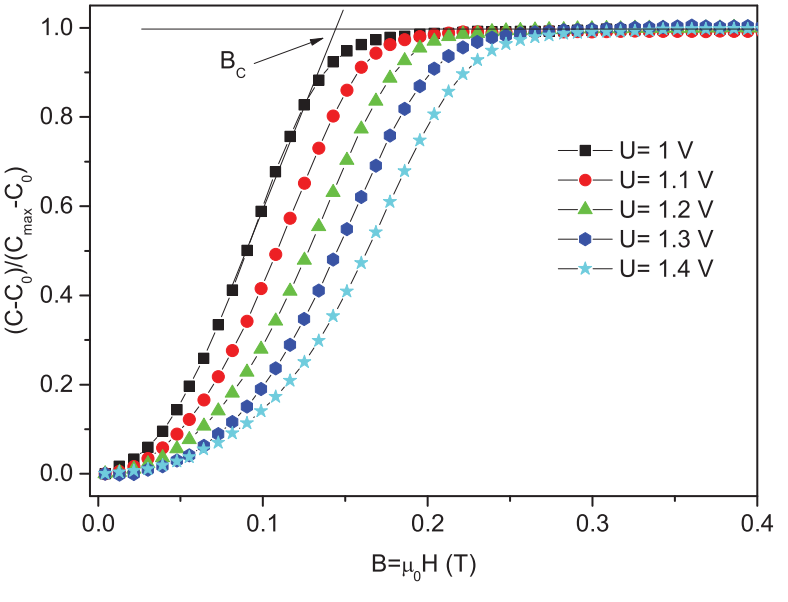

Figure 5. Reduced capacitance vs. the external magnetic field for undoped 6CB measured at various U voltages.

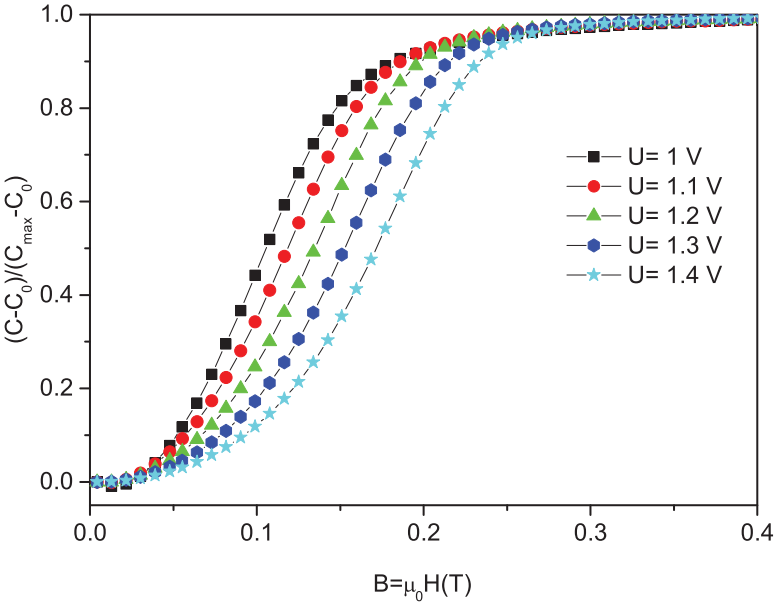

Figure 6. Reduced capacitance vs. the external magnetic field for 6CB doped with spherical MNPs in volume concentration $\phi = 10^{-5}$, measured at various U voltages.

Figure 8 summarizes the data obtained from Figures 5–7, showing how the critical magnetic field B_c (which restores the initial planar alignment) depends on the voltage, for the undoped 6CB as well as for the 6CB based FNs. In the case of the FN with rod-like MNPs, B_c is increased just slightly compared to that of the undoped 6CB, while for the FN with spherical MNPs, the increase is more pronounced. In all cases, the critical magnetic field increases with the increment of U, which is

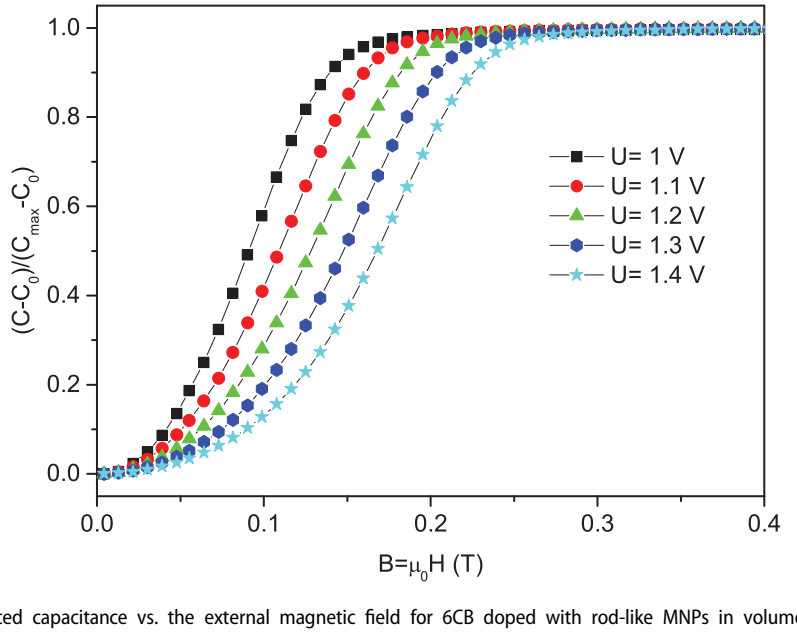

Figure 7. Reduced capacitance vs. the external magnetic field for 6CB doped with rod-like MNPs in volume concentration $\phi = 10^{-5}$, measured at various U voltages.

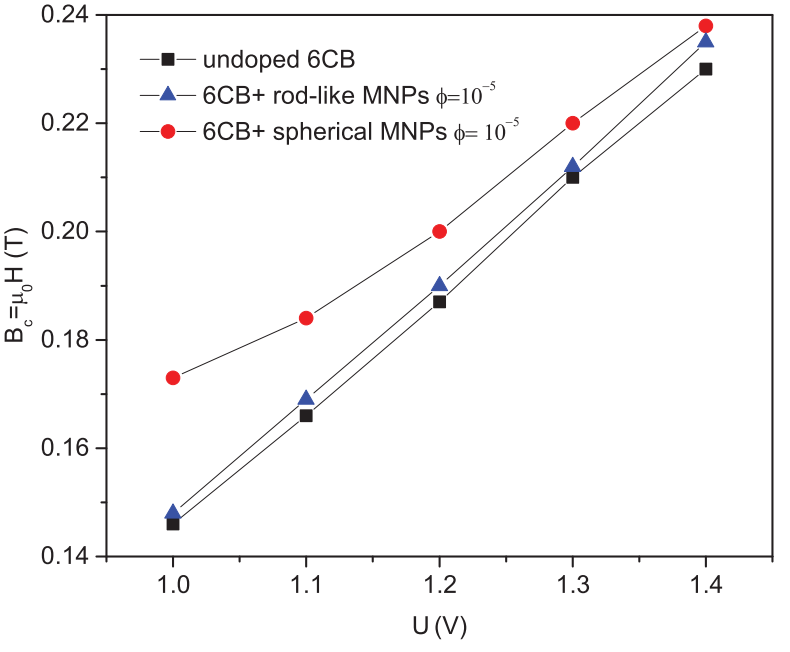

Figure 8. Dependence of the critical magnetic field B_C on the voltage U for the undoped 6CB and for 6CB doped with spherical and rod-like magnetic particles.

understandable: a larger reorienting U requires larger restoring B_c, which is expressed by the relation [16]

$$\left(\frac{U}{U_F}\right)^2 - \left(\frac{B_c}{B_F}\right)^2 = 1. \tag{1}$$

Naturally, Equation (1) holds only for $U \geq U_F$ (for $U < U_F$, there is no structural transition at all). Here B_F is the Fréedericksz threshold induction at $U = 0$ in the same cell, just with the magnetic field normal to the cell surface:

$$B_F = \frac{\pi}{D}\sqrt{\mu_0 \frac{K_1}{|\chi_a|}}. \tag{2}$$

Studying this magnetic Fréedericksz transition, Burylov and Raikher [13] established a theoretical relation between the threshold magnetic induction of thermotropic ferronematics B_{Ffn} and that of the host LC B_F. Under the assumption of a homeotropic anchoring of the LC molecules at the surface of the MNPs, the obtained approximate formula has the form:

$$B_{Ffn}^2 - B_F^2 = \pm \frac{2\mu_0 W\phi}{\chi_a d}. \tag{3}$$

The sign depends on the relative orientation of $\vec{m}$ and $\vec{n}$: it is positive for $\vec{m} \perp \vec{n}$ and is negative for $\vec{m} \parallel \vec{n}$.

The expression for the critical magnetic induction in our experimental geometry directly follows from Equation (1):

$$B_{clc}^2 = B_F^2\left(\frac{U^2}{U_F^2} - 1\right) \text{and } B_{cfn}^2 = B_{Ffn}^2\left(\frac{U^2}{U_{Ffn}^2} - 1\right) \tag{4}$$

for the LC and the FNs, respectively.

Combining Equations (3) and (4), as well as taking into account that $U_F = U_{Ffn}$, one obtains a relation between the critical magnetic fields of the ferronematic (B_{cfn}) and of the host LC (B_{clc}):

$$B_{cfn}^2 - B_{clc}^2 = \pm\frac{2\mu_0 W\phi}{\chi_a d}\left(\frac{U^2}{U_F^2} - 1\right). \tag{5}$$

As both B_{cfn} and B_{clc} were measured, Equation (5) can be used to estimate the anchoring energy density W at the nematic–magnetic particle boundary. The susceptibility anisotropy of 6CB was calculated from Equation (2), yielding $\chi_a = 1.078 \times 10^{-6}$ at $T = 23$ °C. Knowing the concentration of the particles ($\phi = 10^{-5}$) and using the data for different U, one obtains $W \sim 10^{-6}$ N m^{-1} for the rod-like magnetic particles as well as for the spherical MNPs. Now, the parameter $\omega = Wd/K_1$ can also be calculated. As for 6CB, at the measuring temperature, the corresponding elastic constant is $K_1 = 4.4$ pN [29], $\omega \sim 10^{-3} \ll 1$ is obtained for rod-like and $\omega \sim 10^{-2} \ll 1$ for spherical magnetic particles. These values characterize a soft anchoring of the nematic director on the surfaces of the MNPs in 6CB-based FNs, which permits both parallel and perpendicular orientation between the magnetic moment of MNPs and the director. The fact that doping with both spherical and rod-like MNPs increases the critical magnetic field B_c, indicates an $\vec{m} \perp \vec{n}$ initial orientation.

4. Conclusions

Our experimental results indicate soft anchoring at the MNP–LC surface, both in the case of spherical and of rod-like magnetic particles, as a doping material of FNs. The detected soft anchoring permits both parallel and perpendicular orientation between the magnetic moment of MPs and the director. Furthermore, in both the spherical and the rod-like MNP-containing FNs, the critical reorienting magnetic field B_c increased, which strongly implies an $\vec{m} \perp \vec{n}$ initial orientation.

In a previous work [14], the structural transitions were studied in FNs based on the thermotropic nematic LC 4-*n*-octyl-4′-cyanobiphenyl (8CB) doped with spherical MNPs in various volume concentrations: $\phi_1 = 10^{-4}$, $\phi_2 = 10^{-3}$, $\phi_3 = 5\times 10^{-3}$ and $\phi_4 = 10^{-2}$. By capacitance measurements, $\vec{m} \perp \vec{n}$ initial condition was found for these 8CB-based ferronematics. These results are in perfect agreement with our findings on the 6CB-based FNs presented here; the good match is not surprising, since 8CB and 6CB are close members of the same cyano-biphenyl homologous series, differing only by two carbon units in their alkyl chain.

On the other hand, the influence of the shape of MNPs on FN behaviour was studied in ferronematics based on a nematic with different molecular structure, 4-(trans-4′-*n*-hexylcyclohexyl)-isothiocyanatobenzene (6CHBT) [15]. Those experimental results indicated soft anchoring in the case of doping with spherical MNPs and rigid anchoring when the FN contained rod-like or chain-like MNPs. In all three cases, the initial orientation was $\vec{m} \parallel \vec{n}$, which differs from the present results on 6CB.

Based on these findings, we can conclude that both the shape of the MNPs and the type of the host LC are important in determining the anchoring of nematic molecules on the MNP's surface.

Disclosure statement

No potential conflict of interest was reported by the authors.

Funding

This work was supported by projects the Slovak Academy of Science [grant number VEGA 2/0045/13]; Slovak Research and Development Agency [grant numbers APVV-015-0453 and APVV-SK-HU-2013-0009]; Ministry of Education Agency for Structural Funds of EU [grand number 26220120033]; EU FP7M-era.Net - MACOSYS, Hungarian Scientific Research Fund [grant number OTKANN 110672]; the Hungarian National Research, Development and Innovation Office (NKFIH) [grant number TÉT_12_SK-1-2013-0025].

References

[1] Kim KH, Song JK. Technical evolution of liquid crystal displays. NPG Asia Mater. 2009; 1: 29–36.
[2] Palffy-Muhoray P, Cao W, Moreira M, et al. Photonics and lasing in liquid crystal materials, Philos. Transt. A. 2006;364:2747–2761.
[3] Mertelj A, Ostrman N, Lisjak D, et al. Magneto-optic and converse magnetoelectric effects in a ferromagnetic liquid crystal. Soft Matter. 2014;10:9065–9072.
[4] Lagerwall JPF, Scalia G. A new era for liquid crystal research: applications of liquid crystals in soft matter nano-, bio- and microtechnology. Curr Appl Phys. 2012;12:1387–1412.
[5] de Gennes PG. The physics of liquid crystals. Oxford: Clarendon Press; 1974.
[6] Freedericksz V, Zolina V. Forces causing the orientation of an anisotropic liquid. Trans. Faraday. Soc. 1970;29:919–930.
[7] Brochard F, de Gennes PG. Theory of magnetic suspensions in liquid crystals. J Phys France. 1970;31:691–708.
[8] Liebert J, Martinet A. Coupling between nematic lyomesophases and ferrofluids. J Phys Lett. 1979;40:363–368.
[9] Figueiredo Neto AM, Liebert L, Levelut AM. Study of ferrocholesteric discotic and calamitic lyotropics by optical microscopy and X-ray diffraction. J Phys France. 1984;45:1505–1512.
[10] Chen SH, Amer NH. Observation of macroscopic collective behaviour and new texture in magnetically doped liquid crystals. Phys Rev Lett. 1983;51:2298–2301.
[11] Burylov SV, Raikher YL. On the orientation of an anisometric particle suspended in a bulk uniform nematic. Phys Lett A. 1990;149:279–283.
[12] Burylov S. V, Raikher Y. L. Magnetic Fredericksz transition in a ferronematic. J Magn Magn Mater. 1993;122:62–65.
[13] Burylov S. V, Raikher Y. L. Molecular properties of ferronematic caused by orientational interactions on the particle surface. II. Behavior of real ferronematics in external fields. Mol Cryst Liq Cryst. 1995;258:123–141.
[14] Kopcansky P, Koneracka M, Potocova I, et al. The anchoring of nematic molecules on magnetic particles in some types of ferronematics. Czech J Phys. 2001;51:59.
[15] Kopcansky P, Tomasovicova N, Koneracka M, et al. Structural changes in the 6CHBT liquid crystal doped with spherical, rodlike, and chainlike magnetic particles. Phys Rev E. 2008;78:011702–011705.
[16] Tomasovicova N, Kopcansky P, Eber N. Anisotropy research: new developments. Hauppauge (NY): Nova Science; 2012. Chapter 11; p. 245–276.
[17] Mertelj A, Lisjak D, Drofenik M, et al. Ferromagnetism in suspensions of magnetic platelets in liquid crystal. Nature. 2013;504:237–241.
[18] Prodanov MF, Buluy OG, Popova EV, et al. Magnetic actuation of a thermodynamycially stable colloid of ferromagnetic nanoparticles in a liquid crystal. Soft Matter. 2016;12:6601–6609.
[19] Xiang W, Shengli P, Hongzhu J, et al. Enhanced magnetic-field-induced optical properties of nanostructured magnetic fluids by doping nematic liquid crystals. Nanoscale Res Lett. 2012;7: 249/1–7.
[20] Xiang W, Shengli P, Hongzhu P, et al. Optical transmittance of ferronematic materials in the visible range. J Optoelectr Adv Mater. 2014;16:771–775.
[21] Tomasovicova N, Timko M, Mitroova Z, et al. Capacitance changes in ferronematic liquid crystals induced by low magnetic fields. Phys Rev E. 2013;87:014501–014504.
[22] Podoliak N, Buchnev O, Buluy O, et al. Macroscopic optical effects in low concentration ferronematics. Soft Matter. 2011;7:4742–4749.
[23] Buluy O, Nepijko S, Reshetnyak V, et al. Magnetic sensitivity of a dispersion of aggregated ferromagnetic carbon nanotubes in liquid crystals. Soft Matter. 2011;7:644–649.
[24] Gorkunov MV, Osipov MA. Mean-field theory of a nematic liquid crystal doped with anisotropic nanoparticles. Soft Matter. 2011;7:4348–4356.

[25] Gdovinova V, Tomasovicova N, Eber N, et al. Influence of the anisometry of magnetic particles on the isotropic-nematic phase transitions. Liq Cryst. 2014;41:1773–1777.
[26] Tomasovicova N, Timko M, Eber N, et al. Magnetically induced shift of the isotropic-nematic phase transition temperature in a mixture of bent–core and calamitic liquid crystals doped with magnetic particles. Liq Cryst. 2015;42:959–963.
[27] Gray GW, Harrison KJ, Nash J A. New family of nematic liquid crystals for displays. Electron Lett. 1973;9:130–131.
[28] Tomasovicova N, Kovac J, Raikher Y, et al. Biasing a ferronematic a new way to detect weak magnetic field. Soft Matter. 2016;12:5780–5786.
[29] Czechowski G, Czerkas S, Jadzyn J. The elastic constants of nematic n-Hexylcyanobiphenyl determined with the capacitance method. Z Natur Sch. 2001;56:257–261.